Template Growth of ZnO Nanorods and Microrods with Controllable Densities

ARTICLE *in* CRYSTAL GROWTH & DESIGN · JUNE 2008

Impact Factor: 4.89 · DOI: 10.1021/cg7012599

4 AUTHORS, INCLUDING:

Wei Gao
University of Auckland

CRYSTAL GROWTH & DESIGN
2008
VOL. 8, NO. 7
2406–2410

Template Growth of ZnO Nanorods and Microrods with Controllable Densities

Xiaodong Yan, Zhengwei Li, Ruiqun Chen, and Wei Gao*

Department of Chemical and Materials Engineering, The University of Auckland, Private Bag 92019, Auckland, New Zealand

Received December 21, 2007; Revised Manuscript Received March 14, 2008

ABSTRACT: ZnO nanorod/microrod arrays with controllable surface distribution densities were successfully synthesized on glass substrates via a low-temperature template-assisted aqueous solution growth method. The influences of the pH of the solution on the formation and continuing growth of ZnO crystals were studied. It was found that the variation of pH in the reaction system significantly affects the density of homogeneous nucleation on the template surface. With a low surface density of the nanorod arrays, the effects of solution composition on the growth of ZnO crystals can be clearly revealed, and these have been demonstrated with the formation of ZnO nanorods in $Zn^{2+} + Al^{3+}$ + HMT solutions.

1. Introduction

Recently, zinc oxide (ZnO) based nano/microstructures have attracted much attention due to their great potential for fundamental studies and applications in optoelectronic devices such as blue-UV light-emitting diodes, transparent transistors, solar cells, and biomedical sensors.[1–7] The electronic and optical properties of ZnO nano/microstructures are largely dependent on their composition, crystal structure, dimension, and morphology. In particular, low-dimensional ZnO structures with controlled morphology offer great potential in efficient assembly of nanoscale devices.

A number of techniques have been exploited to prepare ZnO nano/microstructures.[8–11] In comparison with physical methods, the wet chemical bath deposition (CBD) has obvious advantages of low-cost, low-temperature operation and environmental friendliness. Currently, ZnO nanorods with different shapes can be prepared using CBD with the assistance of organic chemicals, such as citrate, ethylenediamine, and triethanolamine,[12–16] or in basic solutions with sodium hydroxide.[17] In general, the ZnO nanorods grown by CBD have very high surface distribution densities; therefore, nanorod arrays were actually formed. This, to a large extent, makes it difficult to characterize the structural and functional properties of single nanostructures since the harvest from such a dense nanorod array is not always feasible. Additionally, it is expected that the influences of growth conditions, such as temperature, time, solution concentration, doping, and solution additive on the nucleation and growth of nano/microstructures could be observed with ease if the space between them is larger. However, fabrication of high-quality ZnO nano/microrods with controllable surface distribution densities still remains a challenge.

In the present study, an effective method was developed to control the surface distribution density of ZnO nano/microrods grown on templates by adjusting the initial pH value of the reaction solution. In acidic solutions (pH = 3−5), thin hexagonal ZnO rods were formed with low densities. When the pH was increased to 6−7 in the reaction solution, ZnO rods were formed with high densities, leading to dense array films on the template. The influence of Al^{3+} addition into Zn^{2+} + HMT solution on the growth of ZnO nano/microrods at a solution of pH = 5 was also studied.

* Corresponding author. E-mail: w.gao@auckland.ac.nz.

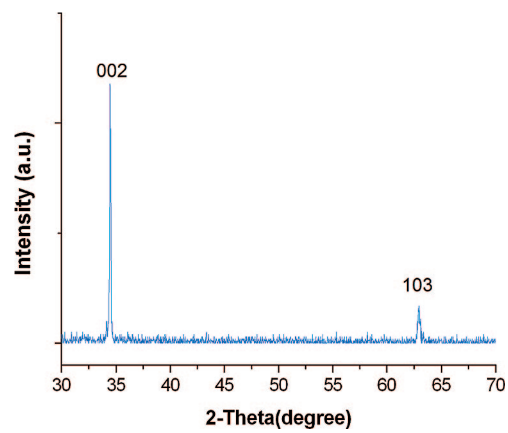

Figure 1. Typical XRD pattern of the as-grown ZnO nano/microrods.

2. Experimental Procedures

2.1. Template Preparation. Glass substrates with a typical size of 15 × 10 × 1 mm were cut from microscope glass slides. They were ultrasonically cleaned in ethanol for 10 min followed by hot air drying. The substrates were then loaded into the chamber of a magnetron sputter. When the deposition chamber was evacuated down to $\sim 5.3 \times 10^{-4}$ Pa, high purity argon with a pressure of 2.67 Pa was introduced into the chamber. Radio-frequency (13.56 MHz) power of 500 W was forwarded to the substrates to initialize plasma for surface cleaning. After that, direct-current power with a density of 0.4 W/cm^2 was forwarded to a ZnO target (99.99%). Deposition was conducted for 30 min to establish a thin ZnO film on the glass substrate.

2.2. Growth of ZnO Nano/Microrods on Templates. Aqueous solutions for the growth of ZnO nano/microrods were prepared using 80 mL of 0.025 mol/L zinc nitrate ($Zn(NO_3)_2 \cdot 6H_2O$, 98%) and hexamethylenetetramine (HMT) ($C_6H_{12}N_4$, 99%) with a molar ratio of 1:1.[18] Diluted nitride acid (HNO_3, 5 mol/L) or ammonia hydroxide (NH_4OH, 5 mol/L) solution was used to adjust the pH value from 3 to 7 to give a clear, colorless solution. The solution was then transferred into a sealable glass bottle in which the glass substrates with ZnO templates were suspended vertically. The sealed bottle was put into an oven at 95 °C for 4 h, after which the glass substrates were withdrawn from the solution, rinsed with DI water, and dried at room temperature.

For the growth of ZnO nano/microrods with $Al(NO_3)_3$ in solution, 80 mL of solution containing 0.025 mol/L $Zn(NO_3)_2$, 0.025 mol/L HMT, and 0.0025 mol/L $Al(NO_3)_3$ were prepared. The initial pH values of the solutions were adjusted to 5 and 7. Growth was carried out at 95 °C for 4 h.

10.1021/cg7012599 CCC: $40.75
Published on Web 06/17/2008

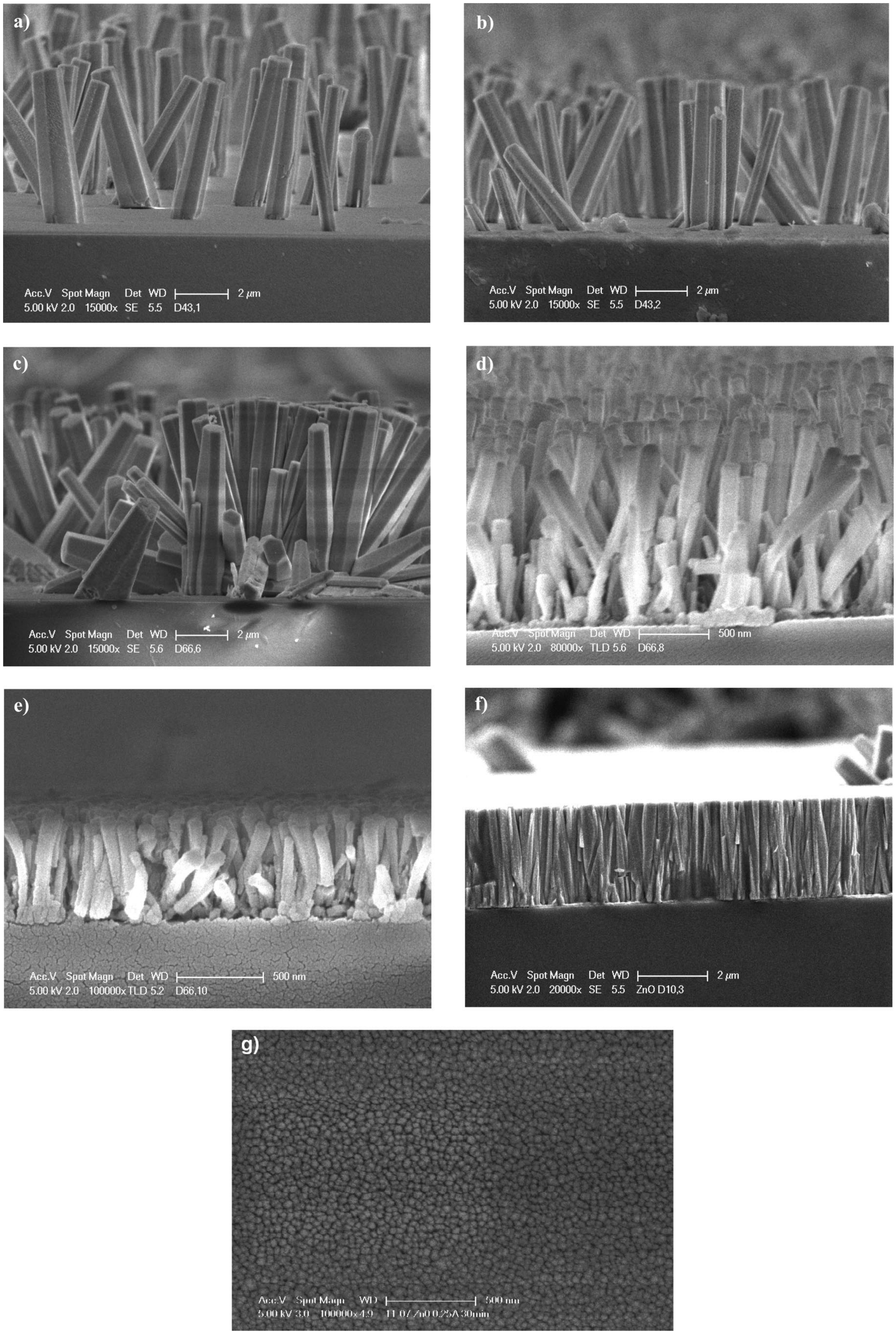

Figure 2. SEM images of as-grown ZnO nano/microrods with various density: (a) initial pH = 3; (b) initial pH = 4; (c) initial pH = 5; (d) initial pH = 6; (e) initial pH = 7; and (f) 0.1 mol/L $Zn(NO_3)_2$ + 0.1 mol/L HMT at pH 6; (g) ZnO seed template deposited by magnetron sputter for 30 min.

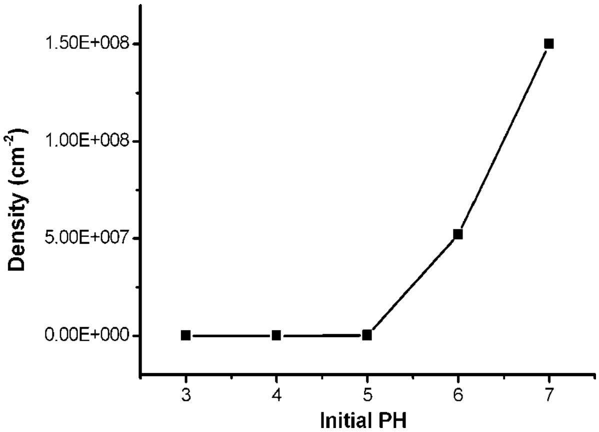

Figure 3. Surface distribution density of ZnO nano/microrods vs initial pH of growth solution (0.025 mol/L $Zn(NO_3)_2$ + 0.025 mol/L HMT, time = 4 h, temperature = 95 °C).

2.3. Characterization. The surface and fracture cross-sectional morphologies of as-grown ZnO nano/microrods were characterized with scanning electron microscopy (Philips XL-30S) operating at 5 kV, while their crystal structure was analyzed with X-ray diffractrometry (Bruker D8) using Cu Kα radiation.

3. Results

3.1. Crystal Structure. Figure 1 shows the typical XRD pattern collected from the nanostructures grown on ZnO template. The two diffraction peaks are indexed to a typical wurtzite ZnO structure. The intensity of ZnO (002) peak is much higher than that of the other ZnO peaks, indicating the preferential growth of nanorods along the *c*-axis vertical to the substrate.

3.2. Morphology and Composition. Morphology of ZnO nano/microrods with different surface distribution densities on the templates was studied with SEM (Figure 2). When the initial pH value of the solution was set at 3, long hexagonal rods (~8 μm) were obtained as shown in Figure 2a. The average aspect ratio of these ZnO rods was around 10, and the surface distribution density is $\sim 2.1 \times 10^4/cm^2$. As the initial pH value increased to 4, ZnO hexagonal rods with an average aspect ratio of 9 and a surface distribution density of $\sim 3.4 \times 10^4/cm^2$ were grown on the substrate (Figure 2b). With a further increase of pH to 5, the average aspect ratio was not changed, while the surface density went up sharply to $\sim 9.1 \times 10^4/cm^2$ (Figure 2c). When the initial pH of the solution increased to 6 and 7, the average aspect ratios slightly decreased to 8 and 7, respectively. And the surface distribution density of the ZnO nanorods increased significantly to $\sim 5.2 \times 10^7/cm^2$ and $\sim 1.5 \times 10^8/cm^2$, almost 3 orders of magnitude higher than those grown in solutions with low pH values (Figures 2d,e and 3). An increase of the concentrations of $Zn(NO_3)_2$ (0.1 mol/L) and HMT (0.1 mol/L) can further increase the surface density of the ZnO nanorods. As revealed in Figure 2f, closely packed ZnO rods developed into a very dense film which is similar to the columnar-structured ZnO films deposited by magnetron sputtering. These results therefore clearly demonstrated that the initial pH value of the solution has important effects on the formation and development of ZnO nanorods grown from the homogeneous ZnO templates. A simple adjustment of pH can vary the surface distribution density of the ZnO nanorods in a large range.

A top view of ZnO seed film which was deposited by magnetron sputter for 30 min is shown in Figure 2g. This micrograph is used to show that the original size of the seed grains are different. The different grains may have different growing rates, resulting in a different density and distribution of the nanorods.

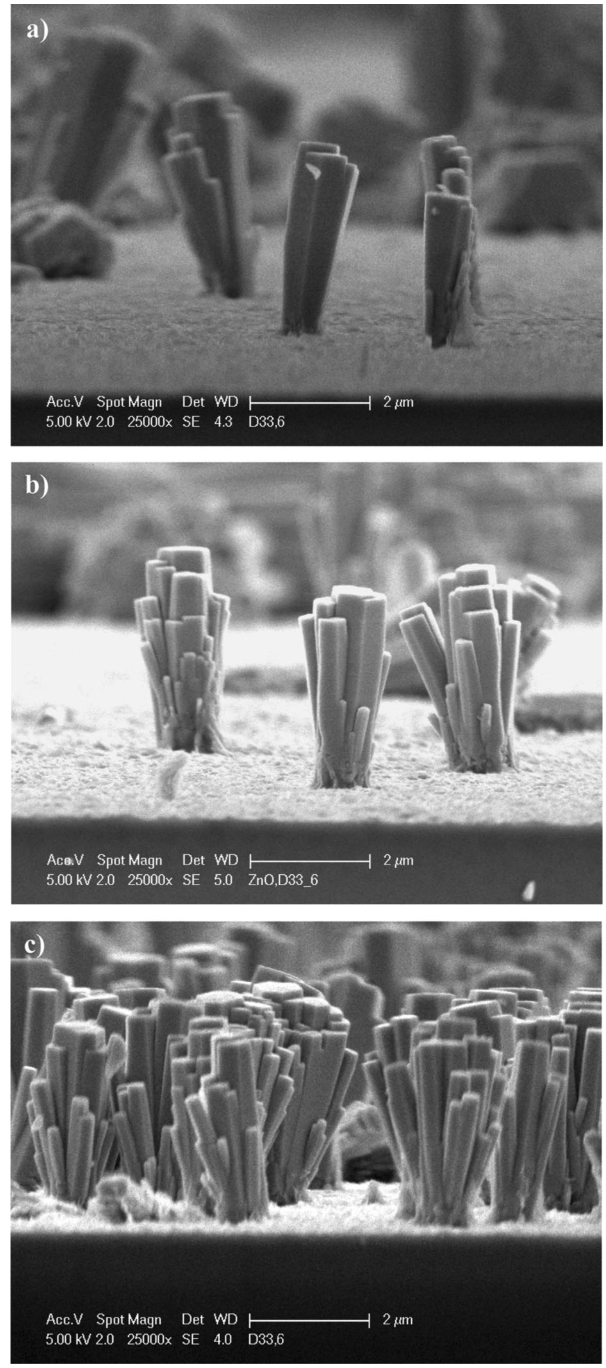

Figure 4. ZnO grown in solutions of containing 0.025 mol/L $Zn(NO_3)_2$, 0.025 mol/L HMT, and 0.0025 mol/L $Al(NO_3)_3$ (time = 4 h, temperature = 95 °C); the initial pH of solution is 5.

It was also found that an addition of 10% $Al(NO_3)_3$ into $Zn(NO_3)_2$ + HMT solution can significantly change the morphological evolution of ZnO nanostructures. From a solution with an initial pH = 5, nanorod clusters were formed (Figure 4). A larger rod was always surrounded by some thinner and shorter rods which were all developed from the large rod's bottom close to the template surface. Observation from the top of the rods revealed that the surface morphology of the sample is very different from that of the samples prepared in Al^{3+} free

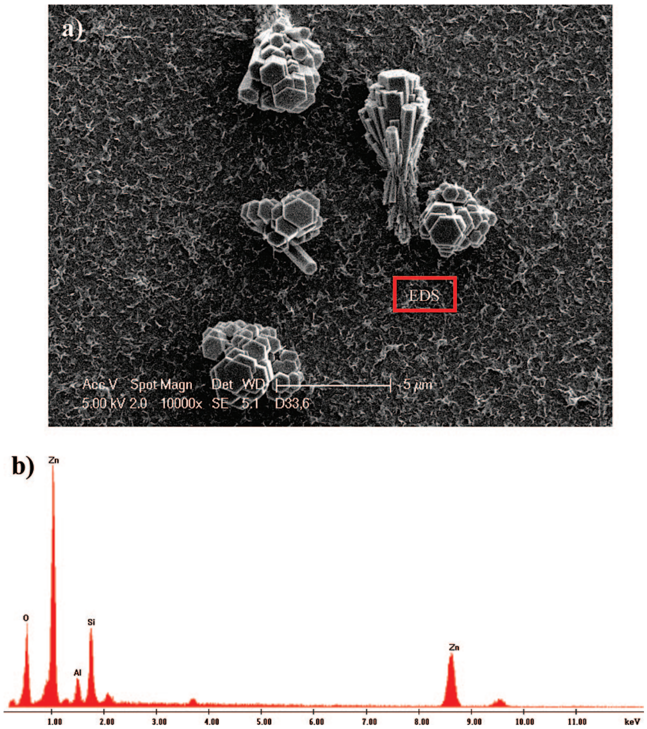

Figure 5. (a) Top view of rod-cluster ZnO nanorods grown from the Zn^{2+} + Al^{3+} + HMT system and (b) compositional analysis of the film covering the surface.

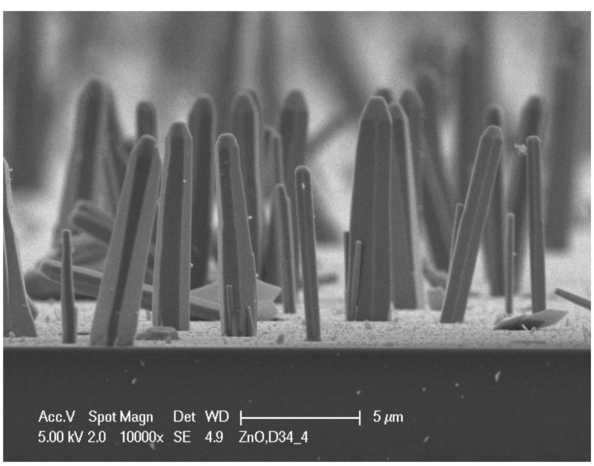

Figure 6. ZnO nanorods with sharp tips grown from 0.02 mol/L $ZnCl_2$ + 0.05 mol/L HMT system. The initial pH of solution is 5.

solution. It appears that a thin layer was covering the ZnO template (Figure 5a). EDS analysis on this layer revealed a high content of Al (Figure 5b). It is then supposed that $Al(OH)_3$ or $Al(H_2O)_6^{3+}$ might form through the reaction between Al^{3+} and H_2O then covered the surface of the template.

Similarly, by using a different zinc precursor, $ZnCl_2$, the morphological change of the discrete ZnO rods could be seen. In comparison with the flat hexagonal top of the rods grown from zinc nitrate, in this solution, pencil-like ZnO rods with a sharp tip were formed (Figure 6). These results indicated that the potential influences of growth conditions on the morphological evolution of ZnO rods could be investigated if the space between the rods could be enlarged.

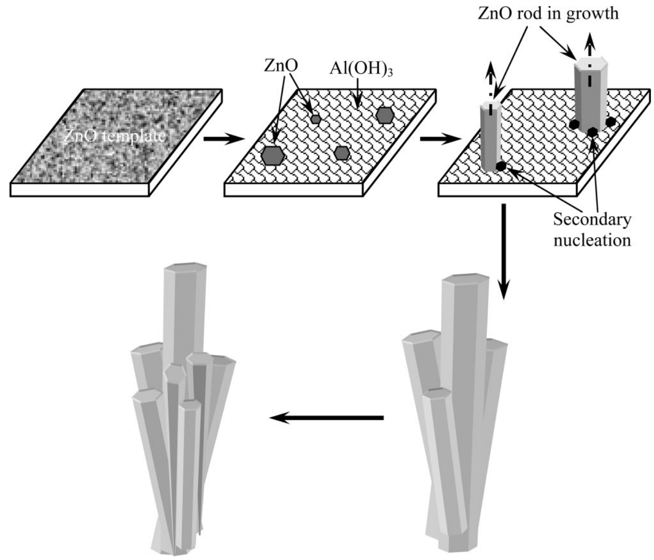

Figure 7. Schematic diagram showing the growth of rod-cluster ZnO in the Zn^{2+} + Al^{3+} + HMT system.

4. Discussion

From the above results, it is clearly seen that ZnO nano/microrod arrays undergo significant density evolution with a change of the initial pH value of the growth solution. To understand the morphological evolution with the variation of solution pH, the chemical reactions involved in the growth of ZnO nanorods on ZnO templates in $Zn(NO_3)_3$ + HMT system at low temperatures will be discussed below:

$$C_6H_{12}N_4 + 6H_2O \rightarrow 4NH_3 + 6HCHO \quad (1)$$

$$H_2O + NH_3 \leftrightarrow OH^- + NH_4 \quad (2)$$

$$Zn^{2+} + 4NH_3 \leftrightarrow Zn(NH_3)_4^{\ 2+} \quad (3)$$

$$Zn^{2+} + 2OH^- \rightarrow Zn(OH)_2 \text{ or } Zn(NH_3)_4^{\ 2+} + 2OH^- \rightarrow Zn(OH)_2(NH_3)_4 \quad (4)$$

$$Zn(OH)_2/Zn(OH)_2(NH_3)_4 \rightarrow ZnO + H_2O \quad (5)$$

With the movement of the reaction equilibrium to the right side, ZnO will form through dehydration of $Zn(OH)_2$ and precipitate onto the template, leading to the formation of ZnO fine structures on the ZnO seeds. Hydrolysis and precipitation reactions in the solutions (eqs 3 and 4) will continuously supply matter for the growth of these structures. This process is similar to the Czochralski technique used for the growth Si single crystals. However, in the solutions with different pH values, the equilibrium of the above reactions may be altered and move in the opposite direction.

When the reactions were carried out in acidic solutions, HMT and H_2O would slowly decompose to generate NH_3, NH_4^+, and OH^- (eqs 1 and 2). The hydrolytic processes (eqs 4 and 5) could still occur since $Zn(OH)_2$ and $Zn(OH)_2(NH_3)_4$) are easily hydrolyzable.[19] ZnO is unstable in an acidic condition; as the size and morphology of ZnO seed particles were different, so the dissolving process and ratio can be different. Figure 2g shows a ZnO seed film deposited by magnetron sputter for 30 min. It can be seen that the grain sizes are different. Some small-sized ZnO nuclei may be dissolved, leading to a significant decrease of nucleus number. This phenomenon has been rationalized in term of slower growth kinetics in the solution with a low pH value.[20,21] Furthermore, some ZnO seeds on the template may be dissolved and disappear during the initial heating period. This would change the uniform distribution of the ZnO seeds after a period of reaction, and then affect the ZnO rods growth afterward.

The growth of ZnO rods is also affected by the crystal habits of wurtzite ZnO. It is well-known that the growth rate of the different family of planes follows the sequence of (0001) > $(10\bar{1}1)$ $(10\bar{1}0)$.[22,23] Consequently, ZnO precipitated from the above reactions would supply mass preferentially to the preferential crystal directions in the existing structures, leading to the formation of discrete but large ZnO vertically aligned rods.

It was reported that the hydroxide precipitation point for the bath containing Zn^{2+} and HMT with a concentration ratio of 1:1 occurs at a pH value of 6.8 at 25 °C,[21] at which the solution is supersaturated. This indicates that ZnO nuclei will form quickly when the initial solution pH value is in the range from 6 to 7. Under this condition, the dissolution of ZnO (seeds or nuclei) will be very limited. Under such a condition, the precipitation reaction will be accelerated and supply a large amount of ZnO for the continuous growth of ZnO structures. As a consequence, thinner ZnO rods will form with a high surface distribution density. These closely packed rods form into dense films with a smaller thickness due to limited mass supplied from the solution in the reaction unit.

In order to find the effect of ZnO seeds template on the growth of ZnO nanostructure, different thicknesses of ZnO seed film were tested in both acidic and neutral solution. By changing the deposition time of sputter (15−40 min), varied thickness ZnO thin films (80−150 nm) were formed. However, after growth of ZnO rods on these templates in the same initial pH condition, the distribution densities of ZnO rods have not shown a significant difference under the current experimental conditions.

A large inter-rod distance provides more opportunity for observation and study of the nanostructure growth. As can be seen from the present results, addition of Al^{3+} into the Zn^{2+} + HMT system greatly modified the growth and morphology of ZnO nanorods in acidic solution (Figure 4). When the pH of the solution is 7, $Al(OH)_3$ precipitation formed immediately and covered the top surface of the ZnO template, thereby inhibiting the growth of ZnO nanorods from the homogeneous ZnO seeds. When the solution pH was lowered to 5, the precipitation of $Al(OH)_3$ was slowed down. Correspondingly, the ZnO template surface might be incompletely covered. Similar to the growth process carried out in the Zn^{2+} + HMT system with a pH value of 5, some ZnO nuclei and seeds would still be dissolved. Precipitation of $Al(OH)_3$ and dissolution of ZnO then largely decreased the sites on the template surface for ZnO crystal growth, leading to the formation of ZnO rods with a significantly reduced surface distribution density (Figure 7).

It is supposed that the formation of the rod-cluster structures is related to the secondary nucleation of ZnO crystals. The crystal structures of ZnO and Al_2O_3 are quite different, and thus the new crystals cannot form on the Al_2O_3 covered surfaces. They then prefer the energy-favorable sites on the existing ZnO rods. Basically, the top (0001) and the bottom (0001) of the rod are preferred sites. On the top of the rod, continuing growth with mass supplied from the solution will be dominated. However, after a certain time period, growth along this direction will be slowed down, evidenced by our observation on the structural evolution of ball-shaped rod clusters.[24] ZnO precipitation thereby has to go to the bottom for nucleation and growth, leading to the formation of cluster-like structures with a larger rod (primary) surrounded by thinner rods (secondary).

5. Conclusions

A strategy has been developed to manipulate the growth of ZnO nanorods and microrods on templates. By adjusting the initial pH value of the aqueous solution containing $Zn(NO_3)_2$ and HMT, ZnO nano/microrods with low to high surface distribution densities have been successfully grown on homogeneous ZnO templates. An increase of the distances between ZnO rods provides a better opportunity to study and understand the nucleation and growth of the ZnO nanoscale structures. Our results also showed that the effect of Al^{3+} addition in $Zn(NO_3)_2$ + HMT solutions on the growth of ZnO rods could be clearly revealed by increasing the inter-rod space through decreasing the solution pH value.

Acknowledgment. This project has been partially supported by a Marsden Fund from the Royal Society of New Zealand. The authors greatly appreciate the technical support from the Department and RCSMS.

References

(1) Wang, Z. L.; Song, J. H. *Science* **2006**, *312*, 242.
(2) Bao, J. M.; Zimmler, M. A.; Capasso, F. *Nano Lett.* **2006**, *6*, 1719.
(3) Huang, M. H.; Mao, S.; Feick, H.; Yan, H. Q.; Wu, Y. Y.; Kind, H.; Weber, E.; Russo, R.; Yang, P. D. *Science* **2001**, *292*, 1897.
(4) Law, M.; Greene, L. E.; Johnson, J. C.; Saykally, R.; Yang, P. D. *Nat. Mater.* **2005**, *4*, 455.
(5) Keis, K.; Vayssieres, L.; Rensmo, H.; Lindquist, S. E.; Hagfeldt, A. *J. Electrochem. Soc.* **2001**, *148*, A149.
(6) Keis, K.; Magnusson, E.; Lindstr, O. H.; Lindquist, S. E.; Hagfeldt, A. *Sol. Energy Mater. Sol. Cells* **2002**, *73*, 51.
(7) Wang, Z. L. *Mater. Today* **2007**, *10*, 20.
(8) Gao, P. X.; Ding., Y.; Mai, W.; Hughes, W. L.; Lao, C.; Wang, Z. L. *Science* **2005**, *309*, 1700.
(9) Greene, L. E.; Law, M.; Tan, D. H.; Montano, M.; Goldberger, J.; Somorjai, G.; Yang, P. D. *Nano Lett.* **2005**, *5* (7), 1231.
(10) Lee, J.; Gao, W.; Li, Z. W.; Hodgson, M.; Metson, J.; Gong, H.; Pal, U. *Appl. Phys. A: Mater. Sci. Process.* **2005**, *80*, 1641.
(11) Jagadish, C.; Pearton, S. *Zinc Oxide Bulk, Thin Films and Nanostructures*; Elsevier: London, 2006.
(12) Tian, Z. R.; Voigt, J. A.; Liu, J. *Nat. Mater.* **2003**, *2*, 821.
(13) Sounart, T. L.; Liu, J.; Voigt, J. A.; Hsu, J. W. P.; Spoerke, E. D.; Tian, Z. R.; Jiang, Y. B. *Adv. Fun. Mater.* **2006**, *16*, 335.
(14) Liu, B.; Zeng, H. C. *Langmuir* **2004**, *20*, 4196.
(15) Greene, L. E.; Yuhas, B. D.; Law, M.; Zitoun, D.; Yang, P. D. *Inorg. Chem.* **2006**, *45*, 7535.
(16) Li, P.; Wei, Y.; Liu, H.; Wang, X. K. *J. Solid State Chem.* **2005**, *178*, 855.
(17) Kawano, T.; Imai, H. *Cryst. Growth Des.* **2006**, *6*, 1054.
(18) Vayssieres, L.; Keis, K.; Lindquist, S. T.; Hagfeldt, A. *J. Phys. Chem.* **2001**, *105*, 3350.
(19) Niesen, T. P.; De-Guire, Mark, R. *Solid State Ionics* **2002**, *151*, 61.
(20) Andres-Verges, M.; Mifsud, A.; Serna, C. J. *J. Chem. Soc. Faraday Trans.* **1990**, *86*, 959.
(21) Govender, K.; Boyle, D. S.; Kenway, P. B.; O'Brien, P. *J. Mater. Chem.* **2004**, *14*, 2575.
(22) Ghoshal, T.; Kar, S.; Chaudhuri, S. *J. Cryst. Growth* **2006**, *293*, 438–446.
(23) Wang, H. H.; Xie, C. S.; Zeng, D. *J. Cryst. Growth* **2005**, *277*, 372–377.
(24) Yan, X. D.; Li, Z. W.; Gao, W., to be published.

CG7012599